

Self-Assembled Polymer Layer with Silver Nanoparticles as an Alternative Coating for Biomedical Applications

Sergio Blanco^{*}, Paula Uribe, Daniela Moreno, Claudia C. Ortiz, Jorge Gutiérrez

Universidad Industrial de Santander, Bucaramanga, Colombia. Calle 9, Carrera 27, ciudad universitaria
 siblanco@uis.edu.co

Healthcare-acquired infections (HAI) have a significant influence in the morbidity and mortality in hospitals. Traditionally, the prevention of the HAI involves two strategies: the use of inert materials, including stainless steel for furniture and equipment, and the disinfection of devices and facilities. In this work, we evaluate a self-assembled polymer layer with silver nanoparticles as an alternative coating on mild carbon steel for the substitution of the more expensive stainless steel and the traditional disinfection procedures. We evaluated the electrochemical response of five different compounds for the self-assembled monolayer (SAM): adipic acid (AA), cysteine (CYS), glycine (GLY), polyethylene glycol (PEG) and polyethylenimine (PEI). The electrochemical stability of the coated steel was evaluated by open circuit potential measurement (OCP), electrochemical impedance spectroscopy (EIS) and linear sweep voltammetry (LSV). For the physicochemical evaluation we used Fourier transform infrared (FTIR), Ultraviolet-visible (UV) spectroscopy and dynamic light scattering (DLS). Then, according to the results we selected the SAMs obtained with adipic acid and glycine to test their assembly with Ag nanoparticles. These coatings were evaluated by electrochemical and microbiological test. The microbiological evaluation of the silver nanoparticles inhibitory effect was performed through a modified microdilution method using *Candidas spp.* The results showed a relationship between the self-assembled layer synthesis procedures and the expected functions that are a low minimal inhibitory concentration (MIC) and the prevention of the corrosion of the mild carbon steel.

1. Introduction

Healthcare-acquired infections (HAI) including pneumonia, gastrointestinal illness, urinary tract infections, primary bloodstream infections and surgical site infections have a significant influence in the morbidity and mortality in hospitals and costs over \$ 28,4 billion dollars each year in the U.S whereas at least a 20 % of them are preventable (Scott, 2009). Furthermore, the situation in Latin America is even worst and worrying since approximately an 11,6 % of hospitalized patients get an HAI while in the U.S only 1,22 % get it. This leads to an increase of patient's expenses up to about \$ 15,275 (Scott, 2009) (Orsi et al, 2002). Moreover, HAI lengthen the hospital stay for at least 7 days (Orsi et al., 2002) (Curcio, 2011). Traditionally, the prevention of HAI involves two strategies: the use of inert materials, including stainless steel for furniture and equipments, and the disinfection of devices and facilities. The disinfection procedures are limited and could be useless depending on the type of microorganisms.

Despite the disinfection and sterilization in healthcare by different techniques (Rutala et al., 2008), the application of new technologies to prevent the bacterial growth has become a necessity. Consequently, the use of nanoparticles (NPs) is a striking option; several assays showed that some metals such as silver and copper have an antimicrobial and antifungal effect (Ahmadi et al, 2013) (Vincent et al., 2016). Ag NPs and some ionic compounds have been used in the last years for their antimicrobial activity when present in coatings, unguents for topical use on burns, water sanitization, etc. (Vivekanandhan et al, 2012). Nowadays, most of equipment of operating room are made of stainless steel, which is an expensive material that requires a tedious cleaning process and is unable to prevent bacterial growth. A possible alternative might be the use of low-price materials such as carbon steel, with special coatings. In this work, we evaluated a self-assembled polymer layer with silver nanoparticles as an alternative coating on mild carbon steel for the substitution of the more expensive stainless steel and the traditional disinfection procedures. We evaluated the response of five

different compounds for the self-assembled layer: adipic acid (AA), cysteine (CYS), glycine (GLY), polyethylene glycol (PEG) and polyethylenimine (PEI), and the influence of the silver nanoparticles on the stability of the coating and the microbial proliferation.

2. Materials and Methods

2.1 Silver nanoparticles synthesis

Sodium bis [2-ethylhexyl] sulfosuccinate (AOT) reverse micelles (RMs) in hexane were formed by mass and volumetric dilution until an optically clear solution was obtained. The amount of solute dissolved in water as reverse micelles is expressed as: $W_s = [\text{solute in water}]/[\text{AOT}]$. All experimental points were measured by triplicate. In all cases, the experimental temperature was kept at $25 \text{ }^\circ\text{C} \pm 0.2 \text{ }^\circ\text{C}$. The synthesis of NanoParticules (NPs) in RMs has been described previously (Gutierrez et al., 2015). The nucleation and growth occurs in a limited space. Thus, two RMs solutions containing -separately- AgNO_3 and H_4N_2 dissolved at the same AOT concentration and W_s were prepared. The reduction process takes place when the two RMs systems are mixed. The concentration used in all systems were $[\text{AOT}] = 0.1 \text{ M}$, $[\text{AgNO}_3] = 0.05 \text{ M}$, $[\text{N}_2\text{H}_4] = 0.3 \text{ M}$

2.2 Characterization of silver nanoparticles

UV/vis spectra were recorded using a spectrophotometer Shimadzu UV-1800. Photon Technology International QM-40 fluorometer equipped with a xenon lamp was used for fluorescent emission measurements. FTIR spectra were obtained using a Bruker Tensor 27 spectrometer, the absorption spectra were obtained by averaging 100 measures with a 0.5 cm^{-1} resolution, using pure hexane as blank and Platinum ATR support. The apparent hydrodynamic diameter (d_{app}) of nanoparticles was determined by dynamic light scattering (DLS) Malvern ZetaSizer Nano-ZS90 with a He-Ne laser of 633 nm. Thirty independent size measurements were made for each individual sample at scattering angle of 90° ; the polydispersity index was always below 0.2. TEM images were obtained using a Transmission Electron Microscopy (TEM) FEI TECNAI G2 STWIN at 20–200 kV with a camera Gatan ES100W and software Gatan Digital Micrograph.

2.3 Antifungal activity of NPs

Antifungal activity of Ag NPs against *C. parapsilosis* ATCC 22019, *C. krusei* A2, *C. glabrata* A2, *C. guillemontii* A2, and *C. albicans* ATCC 10231 were tested according to Clinical and Laboratory Standards Institute guidelines; the minimal inhibitory concentrations (MICs) of the NPs were determined using a broth microdilution method. NPs were added to sterile RPMI-1640 medium containing 2% (w/v) of glucose at pH 7.0. Final concentrations of Ag NPs varied from 34.5 to 0.03 ppm, and the final concentration of tested strains was $1\text{-}5 \times 10^3 \text{ CFU/ml}$. The initial concentration of AOT was 0.1 M, but after dilution in culture media decreased gradually. Finlay, fluconazole was used as negative control and testing was performed in 96-well plates incubated at $35 \text{ }^\circ\text{C} / 48 \text{ hours}$. Optical density (O.D) measurements (performed in triplicate) at 490 nm was used to establish growth curves. The MIC is reported as the lowest concentration of metal NPs able to inhibit growth of the yeasts.

2.4 Self-Assembled Monolayer formation

Commercially available AISI 1020 carbon steel bar (C: 0.17-0.23 %, Mn: 0.3-0.6 %, P<0.04 %, S< 0.05 %) of 12 mm diameter were cut in discs and used as electrode. The discs were polished with sandpaper, cleaned with water and degreased with ethanol in ultrasonic bath. The cleaned specimens were immersed in an aqueous solution containing 60 ppm Cl⁻ and the corresponded organic molecule: adipic acid (AA) 50 ppm, polyethylene glycol (PEG) 50% p/v, cysteine (CYS) 100 ppm, glycine (GLY) 100 ppm and polyethylenimine (PEI) 0.03 % p/v; during 45 mn. The preparation of the SAM-Ag NP assembly was made by immersing the coated steel in the solution of silver nanoparticles during 45 mn.

2.5 Electrochemical Evaluation

The electrochemical stability of the coated steel was evaluated by open circuit potential measurement (OCP), electrochemical impedance spectroscopy (EIS) and linear sweep voltammetry (LSV). A conventional three-electrode cell was used for the analysis, with a platinum wire as a counter electrode and Ag/AgCl electrode as a reference. All the electrochemical measurements were carried out in physiological saline solution. The OCP was measured for 1 h, EIS were evaluated in a frequency range of 0.01 Hz to 10^5 Hz and LSV were measured in the potential range between -30 mV and +300 mV vs open circuit potential at a scan rate of 1 mV/s.

3. Results and discussion

3.1 Physicochemical characterization of the Ag nanoparticles

In order to determine the optical properties of nanoparticles, their form, intensity of wavelength absorption and possible molecular interactions between metal surface and surfactants were assessed by Surface Plasmon Resonance (SPR) and FTIR, respectively and analyzed. Figure 1A shows the absorption spectra of Ag precursor and Ag NPs. The phenomenon observed is the Surface Plasmon Resonance (SPR), corresponding to collective oscillation of free electrons at the surface. SPR spectrum of AgNPs is characterized by a highly intense gaussian band with absorption maximum $\lambda_{\text{absmax}} = 399 \text{ nm}$, typical energy of less than 10 nm NPs in this type of systems (Szunerits et al., 2014). The IR stretching spectra of NPs in AOT RMs suggest interactions of metal surface with polar head of surfactant. We evaluate two different Ws at the same AOT concentration. The changes in intensity and frequency of IR spectra are noticeable as the silver concentration increases. This is due to molecular interactions between silver and the sulfonate group of AOT, specifically between SO_3^- and NPs surface, displacing the Na^+ counter ion revealed by a loss of the splitting between 1221 and 1235 cm^{-1} (Moran et al., 1995). The size of the silver nanoparticles was determined by DLS with a polydispersity index below to 0.2. The nanoparticles obtained proved to be spherical, with a diameter of 6 nm, and monodispersed. This size range is ideal for antifungal applications since it allows preferential effective interactions with microorganisms rather than with phagocytes or other biological species.

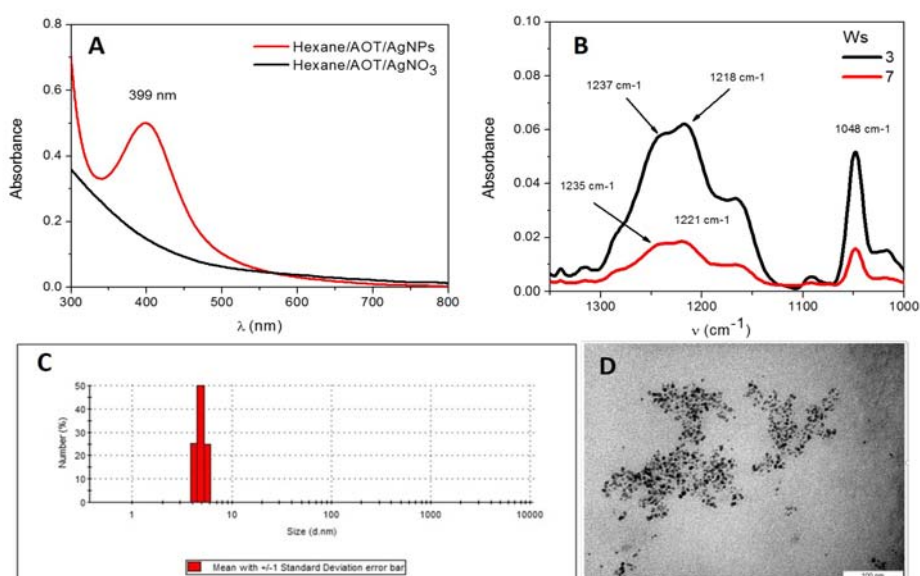


Figure 1. Properties of Ag NPs in hexane/AOT/water. (A) Absorption spectra at Ws=7. Empty RMs were used as blank. (B) Infrared absorption of asymmetric and symmetric S=O stretching at Ws=3 and 7. (C) DLS histogram and (D) TEM image of Ag NPs in hexane/AOT Ws= 7.

3.2 Microbiological evaluation

It has long been known that silver is an excellent antimicrobial agent with fungistatic as well as fungicidal effects (Chen and Schluesener, 2008). The determination of the fungicidal activity of silver nanoparticles was carried out via the assessment of the Minimal Inhibitory Concentration (MIC) using a microdilution method. Growth kinetic was followed at O.D. 490 nm at various time points during 48 hours. Figure 4 shows the inhibition of *Candida* growth from the first addition of Ag NP (0.33 ppm) with an inhibition increasing with the increment of the Ag NP concentration. At 1 ppm, growth of all *Candida* species was totally inhibited. The fungal cell wall contains mannoproteins, β -glucan-chitin and β -glucan and integral proteins, peripheral proteins and ionic channels are embedded into their phospholipidic membrane. The nanoparticles have to interact first with macromolecules of the cell wall before reaching components of the phospholipid membrane. The fungistatic effect of Ag NPs is thought to result from the inhibition of β -glucan synthase and thus cell wall biosynthesis (Romero et al., 2005). In contrast, the fungicidal effect, is thought to be linked to alteration of cell wall integrity. The latter would lose its mechanic resistance, leading osmolytes, ions and metabolites leakage and thus cell destruction (Letscher-Bru and Herbrecht, 2003).

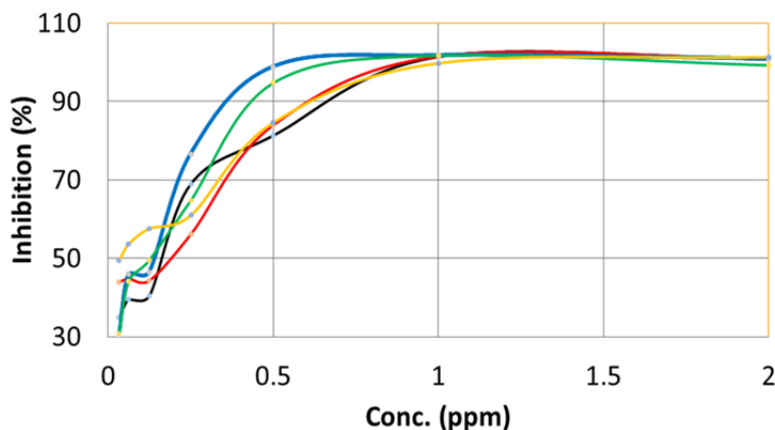


Figure 2. Percentage of growth inhibition of *Candida* spp in function of the silver nanoparticles concentration (ppm). *C. parapsilosis* (black), *C. krusei* (red), *C. glabrata* (blue), *C. guilliermondii* A2 (green).

3.3 Electrochemical evaluation of the surface-modified steel

The electrochemical corrosion of the AISI 1020 carbon steel in physiological solution occurs by anodic dissolution of the iron to produce Fe^{2+} ions. This process takes place homogeneously at the surface. The values of the corrosion potential (E_{corr}) and corrosion current (i_{corr}) were -521 mV vs Ag/AgCl and 3.2×10^{-6} A/cm², respectively. The measured anodic slope (β_a : 84 mV/dec), is in agreement with the theoretical expected value for the transference of two electrons using the Butler-Volmer equation (Bard et al., 1980).

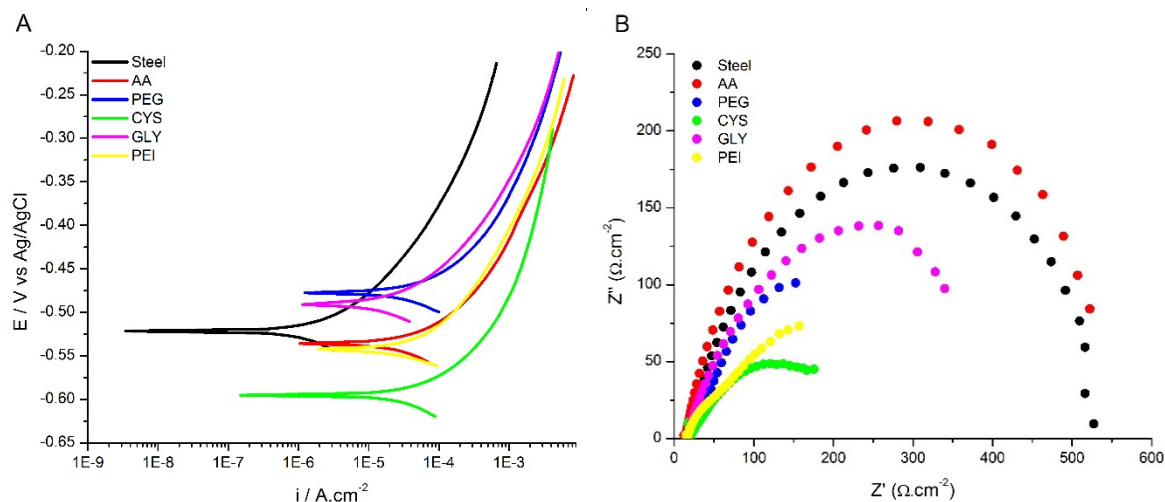


Figure 3. Electrochemical response of the surface-modified steel in physiological solution. (A) linear sweep voltammetry, (B) Nyquist diagram obtained from electrochemical impedance spectroscopy evaluation.

One can conclude from Figure 3 data that the corrosion current was increased 10-20 fold with the surface modification (Table 1). This increment could be related to an increase in the electroactive surface area during the treatment. According to Rajendran (Rajendran et al., 2012), the Cl^- ions present in the solutions used for the modification promote the oxidation of the steel and this oxide interacts with the dissolved molecules to form the self-assembled monolayers. This oxidation process could increase the surface rugosity and the electrochemical active area, resulting in an increment of the measured current. With the surface modification an increment in the anodic slope is observed in comparison with untreated steel. This increment is thought to be due to a reduction of the electrons involved in the reaction during the kinetic controlled oxidation of the steel since the self-assembled layer acts as barrier to reduce ionic exchange with the solution. Nyquist plot (Figure 3B) obtained from the electrochemical impedance spectroscopy analysis shows the variation in the charge transfer resistance (R_{ct}) with the modification of the surface. Considering the simplest equivalent circuit when the capacitance of the double layer (C_{dl}) and the R_{ct} are in parallel, the R_{ct} could be measured from the Nyquist plot by the projection of the semicircle in the Z' axis. The values obtained from the EIS analysis are summarized in Table 1. One notes an apparent reduction in the R_{ct} when a modification of the surface is

obtained with PEG, CYS, GLY and PEI. R_{ct} , as the corrosion current density, depends on the surface area. An increment of the surface area, promoted by the oxidation of the surface during the treatment, results in a reduction of the measured R_{ct} .

Results shown in Figure 3 and Table 1, indicate that the best responses were obtained with adipic acid and glycine. These two molecules were selected to evaluate the absorption of the silver nanoparticles, by assembling steel/AA/Ag NPs and steel/GLY/Ag NPs electrodes. The electrochemical response of these two electrodes in physiological solution are shown in Figure 4. Both systems showed a change in the response obtained by LSV and EIS analysis. The coincidence in the characteristics values obtained for both electrodes (Table 1) is related to the coverage of the surface with the Ag NPs. The values of Tafel slope, charge transfer resistance, corrosion potential and current, correspond to the equilibrium of the silver nanoparticles with the electrolyte. These devices could be useful to avoid microbial growth by two different ways. First, silver nanoparticles attached to the metallic surface inhibits the microbial grown on steel and additionally, the Ag^{2+} liberated by the anodic dissolution limits microbial growth in the surrounding media.

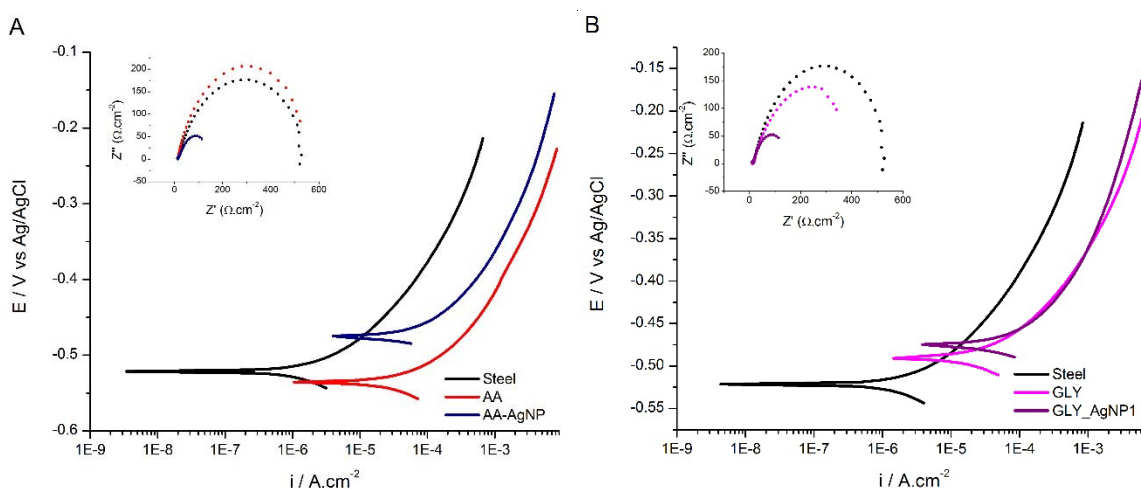


Figure 4. Electrochemical response of the surface-modified steel in physiological solution. (A) LSV and EIS response of the electrode modified with AA-Ag NPs, (B) LSV and EIS response of the electrode modified with GLY-Ag NPs.

Table 1. Characteristic values of the surface modified steel obtained from the electrochemical analysis.

Surface	LSV			EIS
	i_{corr} (A.cm ⁻²)	E_{corr} (mV vs Ag/AgCl)	β_a (mV/dec)	R_{ct} (Ohm.cm ⁻²)
Steel	3,20x10-6	-521	84	528
AA	7,36x10-5	-536	92	547
PEG	8,79X10-5	-478	95	248
CYS	9,56X10-5	-595	105	212
GLY	3,85X10-5	-491	89	410
PEI	6,84X10-5	-542	101	256
AA-Ag NP	1.0x10-4	-475	100	150
GLY Ag NP	1.0x10-4	-475	102	151

4. Conclusions

Monodispersed, spherical (6 nm diameter) silver nanoparticles were obtained by using RM nanoreactor. These particles were highly efficient to limit *Candida spp* growth. They were successfully attached to the surface of steel electrodes *via* their interaction with an intermediary self-assembled monolayer of adipic acid or glycine. These coatings should prove useful to prevent microbial growth on a metallic surface and in the surrounding media.

Acknowledgments

We gratefully acknowledge the financial support for this work at “Estancias Postdoctorales” program of Universidad Industrial de Santander (UIS) and Departamento Administrativo de Ciencia, Tecnología e Innovación (Colciencias), and Universidad Industrial de Santander, Vicerrectoría de Investigación y Extension for funding this Project under internal code 2306.

Reference

- Ahmadi, F., Abolghasemi, S., Parhizgari, N., Moradpour, F., 2013, Effect of silver nanoparticles on common bacteria in hospital surfaces. *Jundishapur journal of microbiology*, 6(3), 209-14, DOI: 10.5812/jjm.4585
- Bard, A. J., Faulkner, L. R., Leddy, J., Zoski, C. G., 1980, *Electrochemical methods: fundamentals and applications* Vol. 2, New York: wiley.
- Chen, X., Schluesener, H. J., 2008, Nanosilver: a nanoparticle in medical application. *Toxicology letters*, 176(1), 1-12, DOI: 10.1016/j.toxlet.2007.10.004
- Curcio, D., 2011, Prevalence of nosocomial infection in Latin American intensive care units. *International Journal of Infection Control*, 7(4), 1-5, DOI: 10.3396/ijic.V7i4.039.11
- Gutierrez, J. A., Luna, M. A., Correa, N. M., Silber, J. J., Falcone, R. D., 2015, The impact of the polar core size and external organic media composition on micelle–micelle interactions: the effect on gold nanoparticle synthesis, *New Journal of Chemistry*, 39(11), 8887-8895 DOI: 10.1039/C5NJ01126D
- Letscher-Bru, V., Herbrecht, R., 2003, Caspofungin: the first representative of a new antifungal class, *Journal of Antimicrobial Chemotherapy*, 51(3), 513-521 DOI: 10.1093/jac/dkg117
- Moran, P. D., Bowmaker, G. A., Cooney, R. P., Bartlett, J. R., Woolfrey, J. L., 1995, Vibrational spectroscopic study of the structure of sodium bis (2-ethylhexyl) sulfosuccinate reverse micelles and water-in-oil microemulsions. *Langmuir*, 11(3), 738-743, DOI: 10.1021/la00003a012
- National Committee for Clinical Laboratory Standards, 2002, Reference method for broth dilution antifungal susceptibility testing of yeasts, approved standard, NCCLS document M27-A2, Wayne, USA.
- Orsi, G. B., Di Stefano, L., Noah, N., 2002, Hospital-acquired, laboratory-confirmed bloodstream infection: increased hospital stay and direct costs, *Infection Control & Hospital Epidemiology*, 23(4), 190-197, DOI: 10.1086/502034
- Rajendran, S., Shribharathy, V., Krishnaveni, A., Sathiyabama, J., Kennedy, Z. R., Banu, V. N., Brintha, G., 2012, Corrosion inhibitive property of self-assembled Nano Films formed by Adipic Acid molecules on carbon steel surface, *Elixir Thin Film Technology*, 50, 10509-10513.
- Romero, M., Cantón, E., Pemán, J., Gobernado, M., 2005, Antifúngicos inhibidores de la síntesis del glucano, *Rev Esp Quimioterap*, 18(4), 281-299.
- Rutala, W. A., Weber, D. J., 2008 Guideline for disinfection and sterilization in healthcare facilities, *Hospital Epidemiology and Division of Infectious Diseases, Centers for Disease Control and Prevention*, <stacks.cdc.gov/view/cdc/11560> accessed 13.10.2017
- Scott, R. D., 2009, The direct medical costs of healthcare-associated infections in US hospitals and the benefits of prevention, *Centers For Disease Control and Prevention*, <stacks.cdc.gov/view/cdc/11550e> accessed 13.10.2017
- Szunerits, S., Spadavecchia, J., Boukherroub, R., 2014, Surface plasmon resonance: signal amplification using colloidal gold nanoparticles for enhanced sensitivity, *Reviews in Analytical Chemistry*, 33(3), 153-164, DOI: 10.1515/revac-2014-0011
- Vincent, M., Hartemann, P., Engels-Deutsch, M., 2016, Antimicrobial applications of copper, *International journal of hygiene and environmental health*, 219(7), 585-591, DOI: 10.1016/j.ijheh.2016.06.003
- Vivekanandhan, S., Christensen, L., Misra, M., Mohanty, A. K., 2012, Green process for impregnation of silver nanoparticles into microcrystalline cellulose and their antimicrobial bionanocomposite films, *Journal of Biomaterials and Nanobiotechnology*, 3(03), 371, DOI: 10.4236/jbnb.2012.33035